

## Vacancy diffusion mediated dynamics of domain boundaries on Ge(111)- $c(2 \times 8)$

Arend-Jan R. Hengst<sup>1</sup>,\* Ying Wang,<sup>1</sup>\* Kevin Vonk<sup>1</sup>, and Harold J. W. Zandvliet<sup>1</sup>†

*Physics of Interfaces and Nanomaterials, MESA<sup>+</sup> Institute, University of Twente, P.O. Box 217, 7500AE Enschede, The Netherlands*



(Received 30 April 2024; accepted 17 June 2024; published 3 July 2024)

Domain boundaries often play a pivotal role in surface dynamics and surface phase transitions. In this study we scrutinize the dynamics of domain boundaries on the Ge(111)- $c(2 \times 8)$  surface using scanning tunneling microscopy. The dynamics of these domain boundaries, which are aligned along the  $\langle 1-10 \rangle$  directions, is governed by the diffusion of vacancies. The hop rate of a vacancy at a domain boundary is more than one order of magnitude larger than the hop rate of a vacancy in a pristine  $c(2 \times 8)$  domain. The diffusion pathway of a single vacancy along the domain boundary involves the formation of two, more mobile, semivacancies. The probability that these two semivacancies rejoin is very likely, but there is also a chance that the two semivacancies diffuse away from each other. This scenario provides a logical explanation of why single vacancies occasionally exhibit unusually long displacements along the domain boundary.

DOI: [10.1103/PhysRevB.110.035406](https://doi.org/10.1103/PhysRevB.110.035406)

### I. INTRODUCTION

The diffusion of atoms and vacancies on surfaces is one of the most elementary and fundamental processes in surface science. For instance, in crystal growth and etching, surface diffusion plays a major role as it governs the roughness and quality of the surface or layers that are grown on, or removed from, the surface [1,2]. Adatom and vacancy diffusion can also play a pivotal role in surface step edge dynamics and surface phase transitions [3].

Among the low-index single crystal surfaces, the Ge(111) surface is an interesting surface that is often used as a model system because of its rather simple adatom-based  $c(2 \times 8)$  surface reconstruction. In the past few decades, the diffusion of adatoms and single vacancies on pristine regions of the Ge(111)- $c(2 \times 8)$  surfaces has been thoroughly investigated using scanning tunneling microscopy [4–6]. In 2004 Brihuega *et al.* [6] demonstrated that the vacancy diffusion on Ge(111) is anisotropic. These authors found that the diffusion barrier of a single vacancy along the  $[1-10]$  direction is  $0.83 \pm 0.03$  eV, whereas the diffusion barrier along the  $[11-2]$  direction is  $0.95 \pm 0.04$  eV [6]. In addition, the attempt frequency in the  $[1-10]$  direction is about a factor of 50 lower than the attempt frequency in the  $[11-2]$  direction [6]. The experimentally obtained diffusion barriers for vacancy diffusion are in very good overall agreement with theoretical calculations by Takeuchi *et al.* [7]. Another study that should also be mentioned here is by Molinàs-Mata *et al.* [5]. In their work, the authors measured the probabilities of several adatom configurations in the vicinity of one or two vacancies. In a follow-up work by Mayne *et al.* [8] the diffusion of single vacancies and pairs of vacancies were studied by scanning tunneling microscopy. The authors concluded that the characteristic diffusion time is

very comparable to the typical time interval between consecutive scanning tunneling microscope (STM) images.

The first scanning tunneling microscopy study on the dynamics of domain walls of the Ge(111) surface was made by Feenstra *et al.* [9]. These authors studied the intricate relation between surface diffusion and the high-temperature order-disorder  $c(2 \times 8)$  to  $(1 \times 1)$  phase transition at 575 K [9]. Einaga *et al.* [10] focused on the role of  $2 \times 1$  domain boundaries on the transition from  $2 \times 1$  to  $c(2 \times 8)$  and Goriachko *et al.* [11] elaborated on the atomistic details of the domain boundaries. However, more studies need to be made dealing with the atomic processes and the diffusion barriers of vacancies/adatoms at the domain boundaries.

Scanning tunneling microscopy is the technique of choice if one wants to study the diffusion of single atoms or vacancies on the atomic scale. Despite the unparalleled spatial resolution, scanning tunneling microscopy also has its disadvantages, such as a low temporal resolution. In the past few decades several groups have developed fast-scanning STMs, so-called video STMs [12,13]. Unfortunately, the high temporal resolution of these video STMs (up to 10–100 images per second) goes at the expense of the spatial resolution. However, other methods to enhance the temporal resolution of a conventional STM exist [14–16]. The most straightforward method to enhance the temporal resolution is to fix the lateral position of the tip and simply record the  $z$ -piezo voltage (feedback enabled) as a function of time [14]. The temporal resolution of this method, which is often referred to as  $z(t)$  spectroscopy, is determined by the cutoff frequency of the feedback electronics and is typically on the order of a few hundred microseconds to 1 ms. Particularly, the combination of conventional scanning tunneling microscopy and  $z(t)$  spectroscopy allows for a thorough study of the elementary atomistic events in surface processes, such as phase transitions, growth, and etching.

Here we focus on the dynamics of domain boundaries on Ge(111)- $c(2 \times 8)$  surfaces at room temperature. We will show that this dynamics is governed by vacancies that diffuse along

\*These authors contributed equally to this work.

†Contact author: [h.j.w.zandvliet@utwente.nl](mailto:h.j.w.zandvliet@utwente.nl)

the domain boundaries, which are aligned to the threefold degenerate  $\langle 1-10 \rangle$  directions of the Ge(111) surface. In addition, we will also demonstrate that the diffusion pathway of a single vacancy is more complex than anticipated. A single vacancy can hop from a stable  $T_4$  site to an adjacent metastable  $T_4$  site, resulting in the formation of two semivacancies. The expression “semivacancy” might appear a bit cryptic, but it will be discussed later; see Figs. 3(a) and 3(b). These semivacancies can either rejoin and form a regular single vacancy again, or diffuse away from each other and form a regular vacancy when they encounter another semivacancy on their way.

## II. EXPERIMENT

The experiments are performed in an ultrahigh-vacuum system with a base pressure below  $3 \times 10^{-11}$  mbar. The ultrahigh-vacuum system is equipped with a room temperature Omicron scanning tunneling microscope (STM-1). The lightly  $p$ -type doped Ge(111) samples, which are purchased from PI-KEM, are mounted on a sample holder that only contains molybdenum, tantalum, and aluminum oxide components. Before inserting the samples into the ultrahigh-vacuum system they are cleaned with isopropyl alcohol. In the ultrahigh-vacuum system the Ge(111) samples are carefully degassed at a temperature of 800 K for at least 24 h. Subsequently, the samples are cleaned by several cycles of argon ion bombardment at 800 eV and annealing at 1100 K via direct current heating. Usually, about ten to 15 of these cleaning cycles are required to obtain clean and well-reconstructed Ge(111)- $c(2 \times 8)$  surfaces [8].

## III. RESULTS AND DISCUSSION

Figure 1(a) shows a large STM image of a Ge(111) surface after several cleaning cycles. In Fig. 1(b) different domains of the reconstructed Ge(111) surface are outlined using different colors. The lowest-energy structure of Ge(111) at room temperature is the centered  $(2 \times 8)$  reconstruction. The  $c(2 \times 8)$  reconstruction is an adatom structure where a quarter monolayer of Ge adatoms is located on top of the Ge atoms of the second layer. These on-top sites are referred to as  $T_4$  sites. The Ge adatoms at these  $T_4$  sites are threefold coordinated to Ge atoms of the unreconstructed underlying Ge(111) substrate. The remaining quarter monolayer of the first layer Ge atoms that are not coordinated to Ge adatoms is referred to as “rest” atoms. The  $c(2 \times 8)$  unit cell of Ge(111) is shown in the left panel of Fig. 1(c). Models of the  $(2 \times 2)$  and  $c(4 \times 2)$  reconstructions are displayed in the right panels of Fig. 1(c). Owing to the hexagonal symmetry of the Ge(111) surface there are three different types of  $c(2 \times 8)$  domains that are invariant under a rotation of  $120^\circ$ . The coexistence of the threefold degenerate  $c(2 \times 8)$  domains and the  $(2 \times 2)$  and  $c(4 \times 2)$  domains results in a plethora of different types of domain boundaries. The most abundant types of domain boundaries are the boundaries between  $c(2 \times 8)$  domains and  $(2 \times n)$  (with  $n = 1$  or  $n \geq 3$ ) domains. These boundaries, which are aligned along the  $\langle 1-10 \rangle$  directions, are dynamic, even at temperatures as low as room temperature.

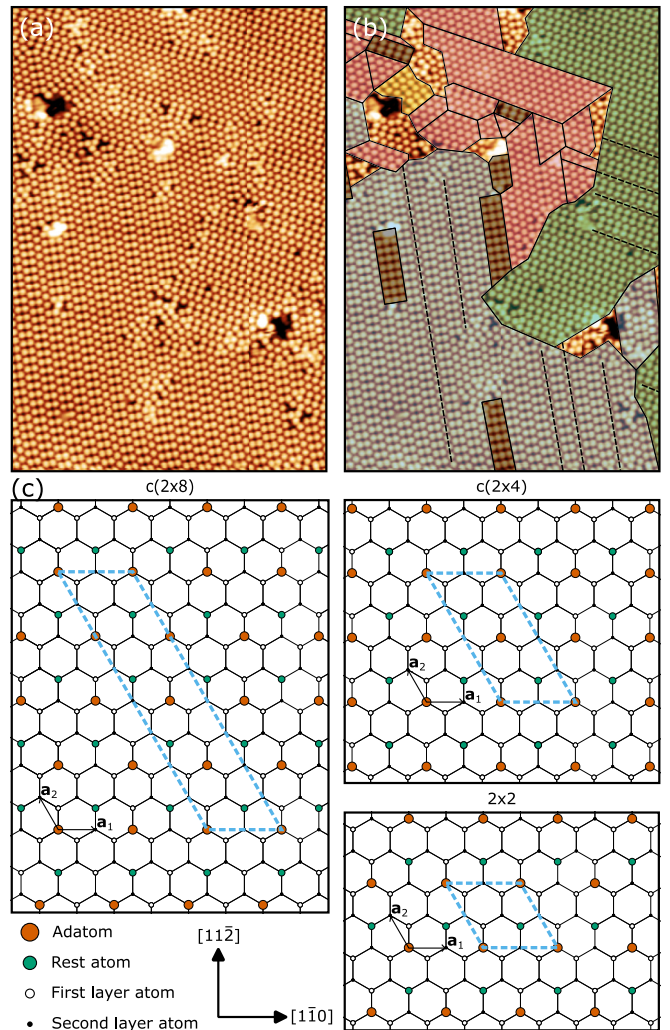


FIG. 1. (a) A  $30 \times 30$ -nm<sup>2</sup> STM topography image of Ge(111) surface at room temperature, recorded with a sample bias of 1.0 V, and a tunnel current of 0.5 nA. (b) The different domains visible in panel (a) are indicated. The  $c(2 \times 8)$  reconstructions are indicated in gray, green, and yellow; the  $c(2 \times 4)$  reconstruction is indicated in black; the  $(2 \times 2)$  reconstruction is indicated in pink; and a local  $(2 \times 2)$  reconstruction within the  $c(2 \times 8)$  reconstruction is indicated using dashed lines. (c) Ball and stick models of the  $c(2 \times 8)$ ,  $c(2 \times 4)$ , and  $(2 \times 2)$  reconstructions.

Figure 2 shows several examples of single vacancies (circles) and semivacancies (half circle), in addition to a more complex arrangement consisting of an adatom and two semivacancies (figure-eight-shaped symbol). The left and right vacancies are located within a  $c(2 \times 8)$  domain, whereas the other two vacancies are located at a phase boundary between two  $c(2 \times 8)$  domains. As shown in Figs. 3(a) and 3(b) a single vacancy can separate into two semivacancies. These semivacancies can either recombine, or diffuse away from each other as shown in Figs. 3(c) and 3(d). When they recombine, there are in principle two options: one of these options does not lead to a net displacement of an adatom (or vacancy), whereas the other option does result in a net displacement of the adatom (or vacancy) by  $8 \text{ \AA}$ . On their journey along the domain boundary semivacancies that diffuse away from each

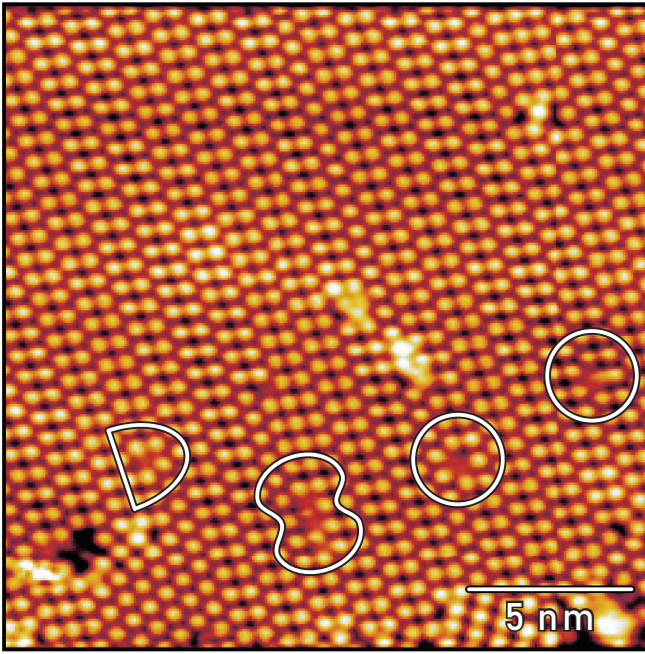


FIG. 2. Topography image of a  $c(2 \times 8)$  reconstructed domain of Ge(111) showing multiple vacancies. The half circle outlines a semivacancy, the circles outline single vacancies, and the figure-eight-shaped symbol shows a dynamic region consisting of two semivacancies and an adatom. The semibright appearance of the vacancies and semivacancies hints at dynamic motion during imaging. The sample bias is 1.0 V and the tunnel current is 0.5 nA.

other can meet other semivacancies and form a regular single vacancy or annihilate at preexisting defects in the domain boundary. As shown in Fig. 3(a) there are two different  $T_4$  sites for adatoms. The two  $T_4$  sites differ in the exact locations of the three neighboring rest atoms. The  $T_4$  adatom site that is located in the center of the three surrounding rest atoms is energetically more favorable than the other  $T_4$  adatom site. Hereafter we will refer to these  $T_4$  sites as the stable and the metastable  $T_4$  adatom site, respectively. The energy difference of a Ge adatom in a stable  $T_4$  site and a metastable  $T_4$  site is estimated in Ref. [5] to be about 50–75 meV. Although we have found several semivacancy pairs in our STM images, we cannot exclude that vacancies (adatoms) can also directly jump from a stable  $T_4$  site to the adjacent stable  $T_4$  site (distance 8 Å).

In Figs. 4(a) and 4(b) two consecutive images are displayed. The time lapse between the images is 316 s. In order to highlight the differences between the two consecutive images, we first register the two images and then subtract them from one another. The resulting difference image is shown in Fig. 4(c). The difference image reveals that the motion takes place exclusively along the domain boundaries, which are aligned along the  $\langle 1-10 \rangle$  directions. In the middle of the difference image there is also a small loop visible. The long black and white trail in the difference image reveals that the vacancy has moved 25 lattice sites (stable  $T_4$  sites) within 316 s. To check if we are dealing with a biased or unbiased one-dimensional (1D) random walk of the vacancy, we have analyzed many domain boundaries and extracted the mean

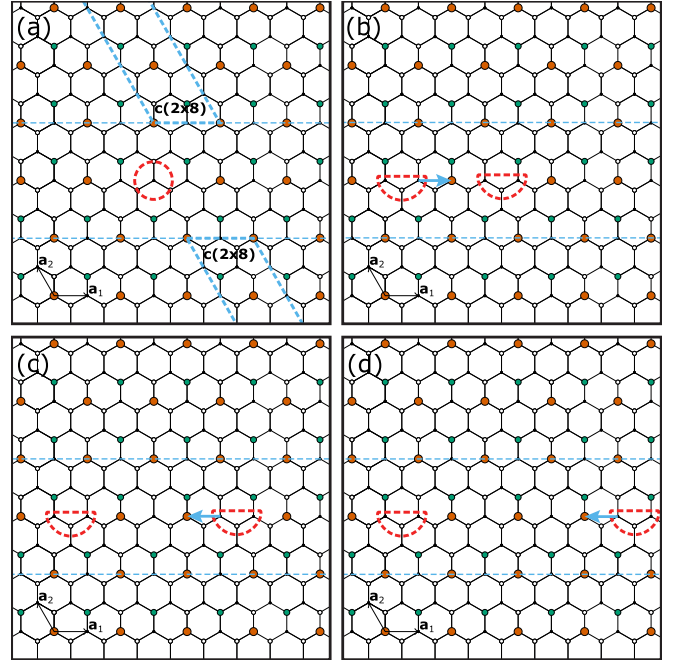


FIG. 3. (a) and (b) Ball-and-stick model of a single vacancy on a Ge(111) surface that separates into two semivacancies. Panels (c) and (d) show two semivacancies that diffuse away from each other in the  $[1-10]$  direction. The dotted red circle and the dotted half circle represent a single vacancy and a semivacancy, respectively. Large gray circles represent Ge adatoms, circles with a dot in the center represent Ge rest atoms, and small gray circles represent Ge atoms of the unreconstructed Ge(111) surface. The  $c(2 \times 8)$  reconstructed domains are outlined by dotted blue lines and the motion of the semivacancies is indicated with blue arrows.

square displacement of single vacancies between successive STM images. In Fig. 5 a plot of the mean square displacement versus time is shown. For an unbiased 1D random walk the mean square displacement ( $\langle x^2 \rangle$ ) scales linearly with time,

$$\langle x^2 \rangle = 2Dt = 2a^2 \nu t = 2a^2 \nu_0 e^{-E_D/k_B T} t, \quad (1)$$

where  $D$  is the diffusion constant,  $a$  the distance between adjacent stable  $T_4$  sites,  $\nu_0$  the attempt frequency,  $E_D$  the diffusion barrier,  $k_B$  the Boltzmann constant,  $T$  the temperature, and  $t$  the time. To compare these results with the diffusion of a vacancy in a pristine  $c(2 \times 8)$  domain we set the jump distance to 8 Å (distance between neighboring stable  $T_4$  sites). The linear dependence of the mean square displacement on time provides compelling evidence that the single vacancy performs a 1D unbiased random walk along the domain boundary. It is worth noting that a 1D random walk of a vacancy along the domain boundary results in a mean square displacement of the domain boundary in a direction normal to the domain boundary that scales as  $\sqrt{t}$  [17]. For more details the interested reader is referred to Ref. [17] and references therein. The average hop rate,  $\nu$  ( $= \nu_0 e^{-E_D/k_B T}$ ), that we extract from the slope of the curve is 0.169 hops per second. This hop rate implies that the average residence time of a vacancy at a stable  $T_4$  site is  $\sim 6$  s. It is important to note that the hop rate of a vacancy in the  $[1-10]$  direction of a pristine  $c(2 \times 8)$  domain is about a factor of 20 lower, resulting in an average

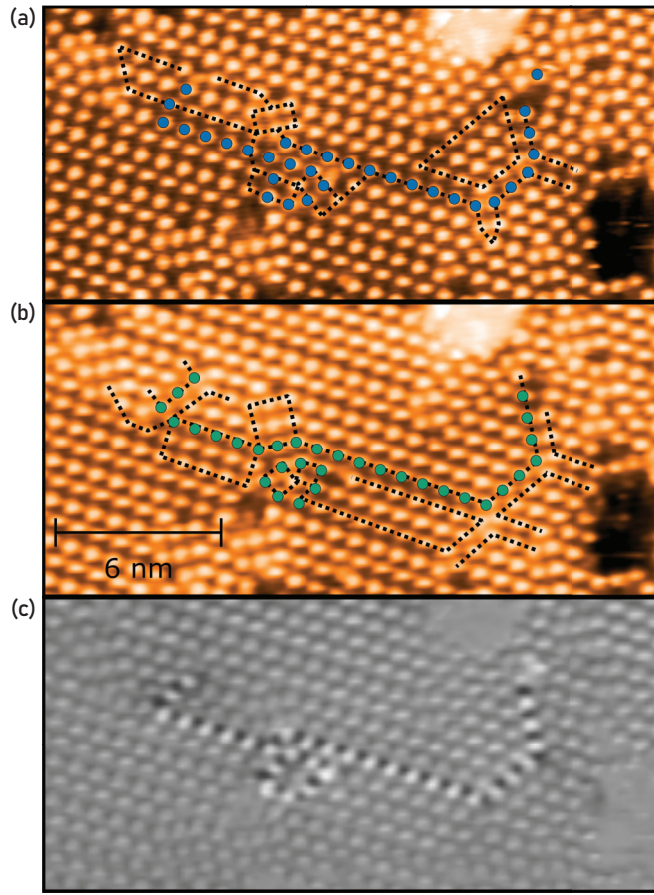


FIG. 4. (a) and (b) Consecutive STM images of the Ge (111) surface at room temperature, recorded with a sample bias of 1.0 V and a tunnel current of 0.5 nA. The time between these two images is 316 s. (c) The difference between the STM images shown in the two top panels. The black and white line shows the motion of the domain boundary.

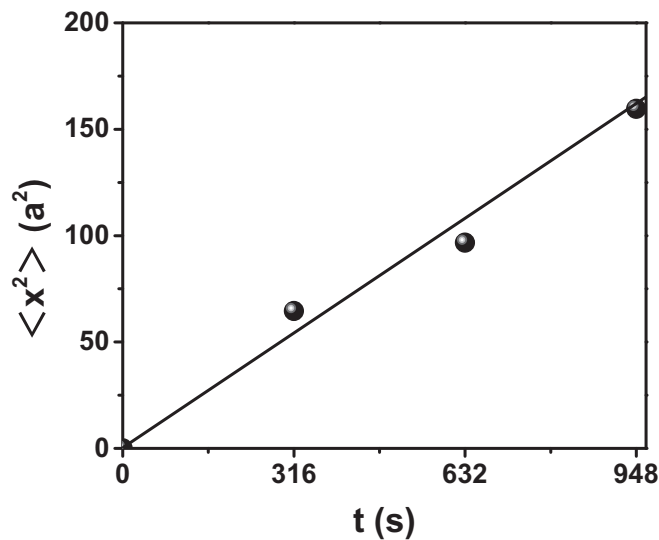


FIG. 5. Mean square displacement of single vacancies that diffuse along (1-10) oriented domain boundaries ( $a = 8 \text{ \AA}$ ).

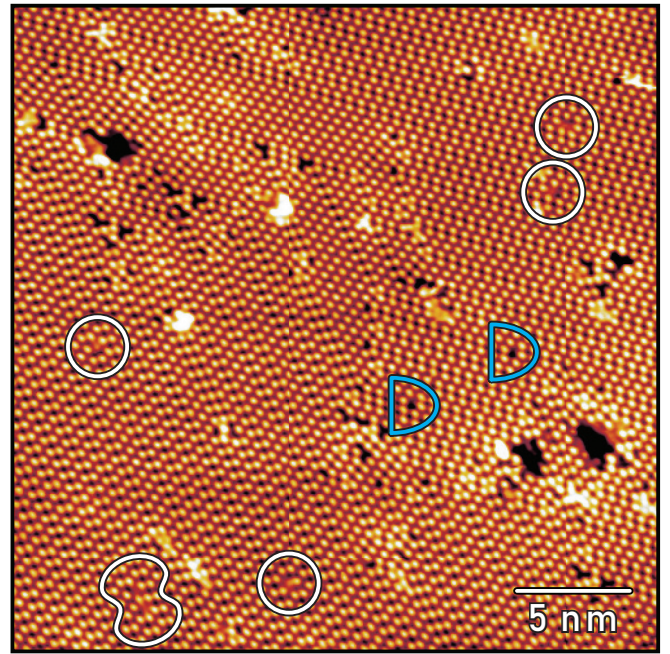


FIG. 6. STM topography images of mobile and immobile single and semivacancies. The figure-eight-shaped symbol outlines a pair of semivacancies. The blue half circles outline type II semivacancies. The circles outline type I single vacancies.

residence time of more than 2 min [6]. The distribution of displacements of vacancies along a domain boundary is not what one would expect for a 1D random walk. The most eye-catching difference is the occurrence of several very long jumps. Statistically, the occurrence of these long jumps is very unlikely. However, as we will see later the occurrence of these long jumps can be understood if we take the formation and diffusion of semivacancies into account.

Before we elaborate on the details of the diffusion of a vacancy we want to emphasize that there are two types of single vacancies and semivacancies, as observed in Fig. 6. Type I vacancies are characterized by a fuzzy appearance, which is caused by motion of the vacancy or semivacancies during imaging. Type II vacancies appear as dark holes with a vanishing intensity. It is very likely that type II vacancies are pinned by defects or impurities in deeper substrate layers.

The dynamics of type I semivacancies is due to hopping of the semivacancy from a  $T_4$  site to a neighboring  $T_4$  site (distance  $4 \text{ \AA}$ ). As the temporal resolution of a STM in its standard scanning mode is insufficient to capture possible, short-lived states, we performed  $z(t)$  measurements. In a  $z(t)$  measurement the STM tip is parked at a location of interest (here a vacancy) and subsequently the  $z$ -piezo displacement is recorded as a function of time with the feedback loop enabled. The temporal resolution of this measurement is determined by the cutoff frequency of the feedback electronics and is estimated to be  $\sim 1 \text{ ms}$ . The diffusion of a vacancy in or out of the tunnel junction will show up as a sudden change in the  $z$  displacement. We have performed these  $z(t)$  measurements at different tunneling conditions, i.e., different sample biases and tunnel currents, in order to check if the observed dynamic events are caused by electrons that tunnel inelastically. We

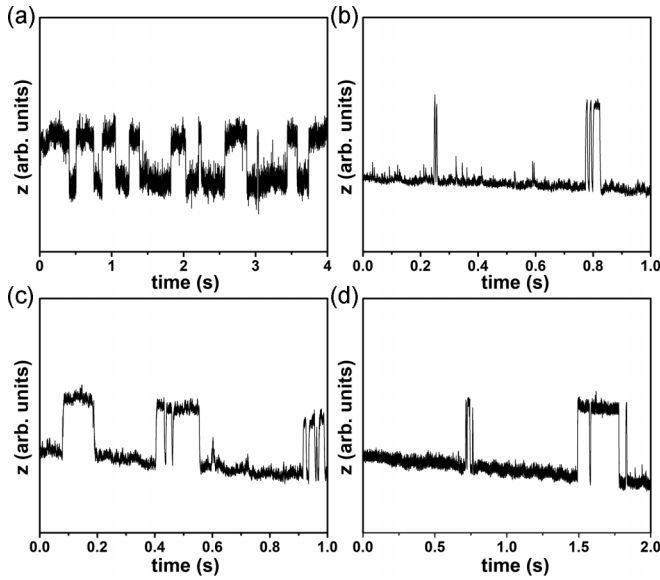


FIG. 7. (a)–(d)  $z$ -piezo voltage recorded at a domain boundary as a function of time with the feedback loop enabled. (a) Sample bias 0.5 V and tunnel current 500 pA, (b,c) sample bias 1.6 V and tunnel current 300 pA, and (d) sample bias 1.0 V and tunnel current 300 pA.

have varied the sample bias from 0.5 to 2 V and the tunnel current from 100 pA to 2 nA and did not find any indication that the tunnel current or sample bias influences the hop rate of the vacancy. This result is not so surprising as Molinàs-Mata *et al.* [5] and Brihuega *et al.* [6] already demonstrated that the diffusion of a vacancy in a pristine  $c(2 \times 8)$  domain is not affected by similar tunnel conditions. In Figs. 7(a)–7(d) typical examples of a  $z$ -piezo displacement trace are shown. There are several hop events in the  $z(t)$  trace of Fig. 7(a), resulting in an average residence time that is much shorter than the expected 6 s. In Figs. 7(b)–7(d) we show several other  $z(t)$  traces. In these traces there are longer time windows where no hopping events occur underneath the tip because the vacancy or semivacancy has diffused away from the tunnel junction. For instance, in Figs. 7(b) and 7(d), a few back and forth jumps in the displacement of the  $z$  piezo are followed or preceded by a longer period where no hopping events are observed. Although there is quite some difference in the residence times of the  $z(t)$  traces shown in the four panels of Fig. 7, it is clear that the average residence time is much smaller than 6 s. We obtain an average residence time of  $\sim 100$  ms, which results in approximately ten hops per second. To explain this huge

discrepancy of a factor of  $\sim 60$  with the hop rate that we extracted from Fig. 5, we propose that the diffusion pathway of a vacancy (adatom) involves an intermediate step where two semivacancies are formed [see Figs. 3(a) and 3(b)]. These semivacancies can quickly rejoin or perform an independent 1D random walk until they meet another semivacancy or annihilate at a defect or one of the two ends of the domain boundary. If there are no semivacancies or defects available in the domain boundary, the semivacancy pair will eventually meet again and form a single vacancy. The average residence time of 100 ms results in a diffusion barrier of about 0.7 eV, assuming an attempt frequency of  $10^{13} \text{ s}^{-1}$ . This diffusion barrier of 0.7 eV for a semivacancy is substantially lower than the 0.83 eV barrier reported for the diffusion of a single vacancy in a pristine  $c(2 \times 8)$  domain [6]. The average lifetime of a semivacancy pair is probably rather short as there is a fair chance that the semivacancy pair rejoins again owing to their attractive interaction [5,8]. The latter results in a decrease of the “effective” attempt frequency for the diffusion of a vacancy from a stable  $T_4$  site to a neighboring stable  $T_4$  site. Two semivacancies can also rapidly diffuse away from each other and recombine with other semivacancies or annihilate at preexisting defects, which provides a natural explanation for the frequently occurring long jumps.

#### IV. CONCLUSIONS

We scrutinize the dynamics of domain boundaries on a Ge(111)- $c(2 \times 8)$  surface and find that the motion of the domain boundaries, which are aligned along the (1-10) directions, is mediated by the diffusion of a vacancy along the domain boundary. We find that the diffusion pathway of a vacancy along a domain boundary involves separation into two semivacancies. This pathway not only explains the discrepancy between conventional scanning tunneling microscopy measurements and  $z(t)$  measurements, but it also explains the occurrence of long jumps of the vacancy along the domain boundary as well as the rather low “effective” attempt frequency.

#### ACKNOWLEDGMENTS

K.V. and H.J.W.Z. acknowledge the research program “Materials for the Quantum Age” (QuMat) for financial support. This program (Registration No. 024.005.006) is part of the Gravitation program financed by the Dutch Ministry of Education, Culture and Science (OCW). Y.W. acknowledges the China Scholarship Council for financial support.

- [1] I. V. Markov, *Crystal Growth for Beginners: Fundamentals of Nucleation, Crystal Growth and Epitaxy* (World Scientific, Singapore, 1995).
- [2] Z. Zhang and M. G. Lagally, *Morphological Organization in Epitaxial Growth and Removal* (World Scientific, Singapore, 1998).
- [3] A. Zangwill, *Physics at Surfaces* (Cambridge University Press, Cambridge, 1998).

- [4] Z. Gai, H. Yu, and W. S. Yang, Adatom diffusion on Ge(111) and the corresponding activation energy barrier, *Phys. Rev. B* **53**, 13547 (1996).
- [5] P. Molinàs-Mata, A. J. Mayne, and G. Dujardin, Manipulation and dynamics at the atomic scale: A dual use of the scanning tunneling microscopy, *Phys. Rev. Lett.* **80**, 3101 (1998).
- [6] I. Brihuega, O. Custance, and J. M. Gómez-Rodríguez, Surface diffusion of single vacancies on Ge(111)- $c(2 \times 8)$  studied by

- variable temperature scanning tunneling microscopy, *Phys. Rev. B* **70**, 165410 (2004).
- [7] N. Takeuchi, A. Selloni, and E. Tosatti, Adatom diffusion and disordering at the Ge(111)- $c(2 \times 8) - (1 \times 1)$  surface transition, *Phys. Rev. B* **49**, 10757 (1994).
- [8] A. J. Mayne, F. Rose, C. Bolis, and G. Dujardin, An scanning tunnelling microscopy study of the diffusion of a single or a pair of atomic vacancies, *Surf. Sci.* **486**, 226 (2001).
- [9] R. M. Feenstra, A. J. Slavin, G. A. Held, and M. A. Lutz, Surface diffusion and phase transition on the Ge(111) surface studied by scanning tunneling microscopy, *Phys. Rev. Lett.* **66**, 3257 (1991).
- [10] Y. Einaga, H. Hirayama, and K. Takayanagi, Role of  $2 \times 1$  domain boundaries on the transition from  $2 \times 1$  to  $c(2 \times 8)$  at Ge(111) surfaces, *Phys. Rev. B* **57**, 15567 (1998).
- [11] A. Goriachko, P. V. Melnik, and M. G. Nakhodkin, New features of the Ge(111) surface with co-existing  $c(2 \times 8)$  and  $(2 \times 2)$  reconstructions investigated by scanning tunneling microscopy, *Ukr. J. Phys.* **60**, 1132 (2015).
- [12] M. J. Rost *et al.*, Scanning probe microscopes go video rate and beyond, *Rev. Sci. Instrum.* **76**, 053710 (2005).
- [13] E. Laegsgaard, L. Österlund, P. Thstrup, P. B. Rasmussen, I. Stensgaard, and F. Besenbacher, A high-pressure scanning tunneling microscope, *Rev. Sci. Instrum.* **72**, 3537 (2001).
- [14] A. van Houselt and H. J. W. Zandvliet, Time-resolved scanning tunnelling microscopy, *Rev. Mod. Phys.* **82**, 1593 (2010).
- [15] B. S. Swartzentruber, Direct measurement of surface diffusion using atom-tracking scanning tunneling microscopy, *Phys. Rev. Lett.* **76**, 459 (1996).
- [16] H. J. W. Zandvliet, B. Poelsema, and B. S. Swartzentruber, Diffusion on semiconductor surfaces, *Phys. Today* **54(7)**, 40 (2001).
- [17] L. Kuipers, M. S. Hoogeman, and J. W. M. Frenken, Step dynamics on Au(110) studied with a high-temperature, high-speed scanning tunneling microscope, *Phys. Rev. Lett.* **71**, 3517 (1993).